Inorg. Chem. **2008**, *47*, 10378−10388

Homogeneous Catalytic System for Photoinduced Hydrogen Production Utilizing Iridium and Rhodium Complexes

Eric D. Cline, Samantha E. Adamson, and Stefan Bernhard*

Frick Laboratory, Department of Chemistry, Princeton University, Princeton, New Jersey 08544

Received May 30, 2008

An efficient homogeneous catalytic system for the visible-light-induced production of hydrogen from water utilizing cyclometalated iridium(III) and tris-2,2′-bipyridyl rhodium(III) complexes is described. Synthetic modification of the photosensitizer $Ir(C^N)_2(N^N)^+$ and water reduction catalyst $Rh(N^N)_3^{3+}$ creates a family of catalysts with diverse photophysical and electrochemical properties. Parallel screening of the various catalyst combinations and photoreaction conditions allows the rapid development of an optimized photocatalytic system that achieves over 5000 turnovers with quantum yields ($^1/_2$ H_2 per photon absorbed) greater than 34%. Photophysical and electrochemical characterization of the optimized system reveals that the reductive quenching pathway provides the necessary driving force for the formation of $[Rh(N^N)_2]^0$, the active catalytic species for the reduction of water to produce hydrogen. Tests for system poisoning with mercury or CS_2 provide strong evidence that the system is a true homogeneous system for photocatalytic hydrogen production.

Introduction

As researchers look for efficient methods to harness renewable clean energy from sustainable sources, hydrogen is a promising candidate as a medium for storage of this energy. Direct conversion of solar energy to chemical energy in the form of hydrogen is an attractive goal that can be accomplished by photosynthetic means from one of Earth's most plentiful resources, water.[1] Designing a complete water-splitting system is a daunting task, and researchers generally develop systems for the oxidative or reductive half-reaction exclusively by replacing the other half-reaction with an appropriate sacrificial reductant (SR) or oxidant.

Photosynthetic methods for hydrogen production from the reduction of water have been examined in several embodiments, including semiconductor-based devices[2,3] and transition metal complexes in heterogeneous[4−10] or homogeneous[11−15] systems. Catalytic systems based on transition-metal complexes involve multiple components, with the distinct advantage that each component can be optimized for its specific task through synthetic modification. The classic example of a heterogeneous system for water reduction uses tris-(2,2′-bipyridine)ruthenium(II), $[Ru(bpy)_3]^{2+}$, as the photosensitizer (PS), methyl viologen as the electron relay (ER), colloidal platinum as the redox mediator, and EDTA as the SR.[4] Heterogeneous systems depend on many parameters that are difficult to control and their potential application in a complete water-splitting system is limited because most heterogeneous catalysts, such as colloidal platinum, promote the recombination of the O_2 and H_2 products. Thus, the

* To whom correspondence should be addressed. E-mail: bern@princeton.edu.

(1) Lewis, N. S.; Nocera, D. G. *Proc. Natl. Acad. Sci. U.S.A.* **2006**, *103*, 15729–15735.
(2) Grätzel, M. *Nature* **2001**, *414*, 338–344.
(3) Khaselev, O.; Bansal, A.; Turner, J. A *Int. J. Hydrogen Energy* **2001**, *26*, 127–132.
(4) Moradpour, A.; Amouyal, E.; Keller, P.; Kagan, H *Nouv. J. Chim.* **1978**, *2*, 547.
(5) Kirch, M.; Lehn, J.; Sauvage, J. *Helv. Chim. Acta* **1979**, *62*, 1345–1384.
(6) Kalyanasundaram, K.; Kiwi, J.; Gratzel, M. *Helv. Chim. Acta* **1978**, *61*, 2720–2730.
(7) Brown, G. M.; Brunschwig, B. S.; Creutz, C.; Endicott, J. F.; Sutin, N. *J. Am. Chem. Soc.* **1979**, *101*, 1298–1300.
(8) Amouyal, E.; Koffi, P. *J. Photochem.* **1985**, *29*, 227–242.
(9) Du, P.; Schneider, J.; Jarosz, P.; Zhang, J.; Brennessel, W.; Eisenberg, R. *J. Phys. Chem. B* **2007**, *111*, 6887–6894.
(10) Tinker, L.; McDaniel, N.; Curtin, P.; Smith, C.; Ireland, M.; Bernhard, S. *Chem.—Eur. J.* **2007**, *13*, 8726–8732.
(11) Krishnan, C. V.; Brunschwig, B. S.; Creutz, C.; Sutin, N. *J. Am. Chem. Soc.* **1985**, *107*, 05–2015.
(12) Brewer, K. J.; Murphy, W. R.; Moore, K. J.; Eberle, E. C.; Petersen, J. D. *Inorg. Chem.* **1986**, *25*, 2470–2472.
(13) Goldsmith, J. I.; Hudson, W. R.; Lowry, M. S.; Anderson, T. H.; Bernhard, S. *J. Am. Chem. Soc.* **2005**, *127*, 7502–7510.
(14) Rau, S.; Schäfer, B.; Gleich, D.; Anders, E.; Rudolph, M.; Friedrich, M.; Görls, H.; Henry, W.; Vos, J. G. *Angew. Chem., Int. Ed.* **2006**, *45*, 6215–6218.
(15) Fisher, J. R.; Cole-Hamilton, D. J. *J. Chem. Soc., Dalton Trans.* **1984**, 809–813.

10.1021/ic800988b CCC: $40.75
Published on Web 10/22/2008

development of efficient homogeneous photocatalytic systems for water reduction is of considerable importance to advance the science of artificial photosynthesis.

Various examples of homogeneous systems have been developed utilizing Co(II),[11−13] Pd(II),[14,15] and Fe_2S_2[16,17] complexes as the water reduction catalyst (WRC), which stores reducing equivalents and carries out the reduction of protons to H_2, without the need for an additional ER. Recently, it was demonstrated that heteroleptic Ir(III) complexes were superior to $[Ru(bpy)_3]^{2+}$ as the PS in systems utilizing tris-(2,2′-bipyridine)cobalt(II), $[Co(bpy)_3]^{2+}$, as the WRC, and triethanolamine (TEOA) as the SR.[13,18] In the Ir−Co system, the Co(II) WRC was the weak component with catalyst instability leading to rapid system deterioration and limiting the overall efficiency of the system.

Tris-(2,2′-bipyridine)Rh(III), $[Rh(bpy)_3]^{3+}$, is an ideal candidate for the WRC component in homogeneous systems because it accumulates two electrons at a suitable potential for water reduction and is known to form hydrides.[19] Additionally, the one-electron reduction product, $[Rh(bpy)_3]^{2+}$, is kinetically unstable and rapidly self-disproportionates to form the doubly reduced species, eliminating the need for a concerted two-electron reduction by the PS.[20] Tris-(2,2′-bipyridine)Rh(III) complexes have been implemented in a two-component homogeneous system for the photoreduction of water with UV irradiation in the presence of TEOA.[5,21] Water reduction using visible-light irradiation of $[Ru(bpy)_3]^{2+}$ with $[Rh(bpy)_3]^{3+}$ in three-component homogeneous systems was unsuccessful in thorough investigations by Sutin and co-workers;[20,22] however, Lehn and coworkers reported one instance of H_2 production using a large excess of the Rh−WRC, which only achieved 12 turnovers (TON, 0.5 H_2 per PS or WRC).[5] During the completion of our own investigations with Rh−WRCs, Brewer and coworkers reported the use of Rh−diimine complexes as the WRC component in a supramolecular system achieving 30 TON,[23] confirming the discoveries that are described in the present account.

The natural photosynthetic machinery harvests visible light to drive water-splitting using a series of finely tuned chromophoric and redox active sites. This complex system is difficult to replicate through artificial systems due to technology, time, and resource constraints. In an attempt to rapidly develop diverse photocatalysts, our group recently used combinatorial techniques to synthesize and study a series of ionic luminophores, bis-(2-phenylpyridine)-(2,2′-bipyridine)iridium(III) $[Ir(ppy)_2(bpy)]^+$, and derivatives thereof that exhibit a wide range of photophysical and electrochemical properties.[24] The efficiency of these complexes as PSs in a homogeneous photocatalytic water reduction system with $[Co(bpy)_3]^{2+}$ was studied, yet no direct correlation existed between photophysics or electrochemistry and catalytic activity.[13,18] This emphasizes the difficulties associated with improving such complex catalytic systems based on physical properties because differences in catalyst activity could be from any combination of changes in light absorption, electron transfer rates, or catalyst stability.

Herein, we describe a new homogeneous system for visible-light-induced hydrogen production from water that utilizes cyclometalated Ir(III) as the PS and tris-2,2′-bipyridyl Rh(III) complexes as the WRC catalyst. Synthetic modification allows the development of a group of catalysts with diverse ground-state and excited-state redox properties. Parallel screening of the structure−activity relationships for the various PS−WRC catalyst combinations, along with optimization of the reaction conditions, leads to the most productive homogeneous photocatalytic system for water reduction to date. Experimental results coupled with photophysical and electrochemical characterization of the optimized system provides insight into the catalytic mechanisms responsible for the photocatalytic reduction of water in this new system.

Experimental Procedure

General. ^{1}H NMR and ^{13}C NMR were recorded on a Varian Inova or Bruker BioSpin Avance II 500 MHz spectrometer at room temperature. ^{19}F-NMR spectra were recorded on a Varian Mercury-VX 300 MHz spectrometer at room temperature. Mass spectral data were collected using a Hewlett-Packard 5898B mass spectrometer or a Kratos MS50TC RF-High Resolution mass spectrometer. Elemental analyses were conducted by the Microanalytical Laboratory at the University of Illinois, Urbana−Champaign.

Materials. 2-Phenyl-pyridine (ppy), 2,2′-bipyridine (bpy), 5,5′-dimethyl-2,2′-bipyridine (dmbpy), 4,4′-di-*tert*-butyl-2,2′-bipyridine (dtbbpy), and 1,2-bis-(diphenylphosphino)ethane (dppe) were purchased from Aldrich. $RhCl_3 \cdot 2H_2O$ and $IrCl_3 \cdot 4H_2O$ were purchased from Pressure Chemical Company. TEOA, triethylamine (TEA), and *N*,*N*′-dimethylaniline (DMA) were purchased from Alfa Aesar. All synthesis and purification solvents were purchased from EM Science. Acetonitrile (ACN), tetrahydrofuran (THF), and *N*,*N*′-dimethylformamide (DMF) for photoreactions were purchased from Acros. Commercial materials were used as received.

5-Methyl-2-(4-methoxyphenyl)pyridine (MeO-mppy), 5-methyl-2-(4-fluorophenyl)pyridine (f-mppy), and 5-(trifluoromethyl)-2-(2,4-difluorophenyl)pyridine (df-CF_3ppy) cyclometalating ligands were synthesized by a Kröhnke pyridine synthesis according to literature procedure.[18,24] The ligand 5,5′-dimethoxy-2,2′-bipyridine (dMeObpy) was prepared by a nickel-catalyzed homocoupling as described in the literature, and the novel compound 5,5′-difluoro-2,2′-bipyridine (dfbpy) was synthesized in a similar manner as described in the Supporting Information.[25]

Tetrakis-(C^N)-μ-(dichloro)diiridium(III) complexes were prepared with the appropriate cyclometalating ligand (C^*N* = ppy,

(16) Na, Y.; Wang, M.; Pan, J.; Zhang, P.; Akermark, B.; Sun, L *Inorg. Chem.* **2008**, *47*, 2805–2810.
(17) Li, X.; Wang, M.; Zhang, S.; Pan, J.; Na, Y.; Liu, J.; Akerman, B.; Sun, L. *J. Phys. Chem. B* **2008**, *112*, 8198–8202.
(18) Lowry, M. S.; Goldsmith, J. I.; Slinker, J. D.; Rohl, R.; Robert, A.; Pascal, J.; Malliaras, G. G.; Bernhard, S *Chem. Mater.* **2005**, *17*, 5712–5719.
(19) Sutin, N.; Creutz, C.; Fujita, E. *Comments Inorg. Chem.* **1997**, *19*, 67–92.
(20) Chan, S.; Chou, M.; Creutz, C.; Matsubara, T.; Sutin, N. *J. Am. Chem. Soc.* **1981**, *103*, 369–379.
(21) Kalyanasundaram, K *Nouv. J. Chim* **1979**, *3*, 511–515.
(22) Brown, G. M.; Chan, S. F.; Creutz, C.; Schwarz, H. A.; Sutin, N. *J. Am. Chem. Soc.* **1979**, *101*, 7638–7640.
(23) Elvington, M.; Brown, J.; Arachchige, S.; Brewer, K. *J. Am. Chem. Soc.* **2007**, *129*, 10644–10645.
(24) Lowry, M. S.; Hudson, W. R.; Pascal, R. A.; Bernhard, S. *J. Am. Chem. Soc.* **2004**, *126*, 14129–14135.
(25) Fukuda, Y.; Seto, S.; Furuta, H.; Ebisu, H.; Oomori, Y.; Terashima, S. *J. Med. Chem.* **2001**, *44*, 1396–1406.

f-mppy, MeO-mppy, and df-CF_3ppy) followed by cleavage with the appropriate neutral ligand (N^N = bpy, dmbpy, dppe, dtbbpy) as described previously to form the series of $[Ir(C^N)_2(N^N)]^+$ products.[18,24,26] The complex $[Co(bpy)_3]Cl_2$ was prepared according to literature procedure.[13] $[Rh(N^N)_3]^{3+}$ where (N^N = bpy, dfbpy, dMeObpy, dtbbpy) was synthesized by a modification of literature procedure.[27] The synthesis, purification, and characterization of the title compounds $[Ir(f\text{-}mppy)_2(dtbbpy)](PF_6)$ and $[Rh(dtbbpy)_3](PF_6)_3$ are described below. All other synthetic notes and structural information are reported in the Supporting Information.

Synthesis of [(4,4′-Ditert-butyl-2,2′-bipyridine)-bis-(2-(4-fluorophenyl)-5-methyl-pyridine)-iridium(III)] Hexafluorophosphate. To $[(f\text{-}mppy)_2Ir\text{-}\mu\text{-}Cl]_2$ (383.8 mg, 300 μmol) and dtbbpy (161.0 mg, 600 μmol) was added ethylene glycol (5 mL), and the reaction was heated at 120 °C under N_2 for 24 h. The cooled reaction mixture was diluted with H_2O (50 mL) and washed with Et_2O (3 × 25 mL). After counterion metathesis with NH_4PF_6(1.0 g in H_2O), the solids were isolated by vac filtration, washed with water, and dried under high vac overnight. The crude product was purified by recrystallization from ACN to produce $[Ir(fmppy)_2(dtbbpy)](PF_6)$ as a yellow cubic crystal in 81% yield.

^{1}H NMR (500 MHz, acetone-d_6): δ 8.88 (d, 2 H, J = 2.0), 8.12 (d, 2 H, J = 8.5), 8.04 (d, 2 H, J = 6.0), 7.94 (dd, 2 H, J = 8.5, 6.0), 7.82 (dd, 2 H, J = 8.5, 1.5), 7.74 (dd, 2 H, J = 6.0, 2.0), 7.48 (d, 2 H, J = 1.5), 6.80 (td, 2 H, J = 9.5, 2.5), 5.93 (dd, 2 H, J = 9.5, 2.5), 2.11 (s, 6 H), 1.43 (s, 18 H).

Synthesis of [Tris-(4,4′-ditert-butyl-2,2′-bipyridine)-rhodium(III)] Tris-hexafluorophosphate. To $RhCl_3 \cdot 2H_2O$ (250 mg, 1.0 mmol) and dtbbpy (808 mg, 3.0 mmol) was added EtOH (10 mL) and H_2O (10 mL), and the reaction was heated at 80 °C for 15 min. We added 1.0 mL of a 1 M solution of hydrazine in EtOH/H_2O and then continued heating at 80 °C for an additional 1 h. Following counterion metathesis with NH_4PF_6 (1.0 g in H_2O), the reaction mixture was concentrated to 10 mL volume by rotary evaporation. The solids were isolated vac filtration, washed with water, and dried under high vac overnight. The crude product was purified by vapor diffusion recrystalization (acetone/pentane) to give $[Rh(dtbbpy)_3](PF_6)_3$ as a white crystalline solid in 74% yield.

^{1}H NMR (500 MHz, acetone-d_6): δ 9.07 (d, 6 H, J = 2.0), 7.90 (d, 6 H, J = 6.0), 7.82 (dd, 6 H, J = 6.0, 2.0), 1.41 (s, 54 H). ^{13}C NMR (125 MHz, acetone-d_6): δ 169.0, 156.0, 151.1, 128.5, 125.5, 37.0, 30.2. MS (*m*/*e*, ESI): 302 (67.5, M^{3+}), 453 (8.7, M^{2+}), 525 (24.1, M^{3+} - PF_6^-). Elem. Anal. Calcd for $C_{54}H_{72}N_6Rh(PF_6)_3$: C, 48.29; H, 5.40; N, 6.26. Found: C, 48.11; H, 5.20; N, 6.29.

General Procedures for Photogeneration of Hydrogen. To evaluate the activity of different catalysts in relationship to one another, all reactions were composed in a uniform fashion through the use of stock solutions prepared using volumetric techniques to reduce the error associated with distributing such small quantities of catalysts. Samples were prepared in 40 mL EPA vials with the appropriate PS, WRC, SR, and solvent as defined for each set of experiments. Reactions were prepared by distributing a stock ACN solution of catalyst to ensure uniformity between reactions. These samples were immediately concentrated to dryness by rotary evaporation before adding 10 mL of the appropriate reaction media. Alternatively, stock solutions of $[Ir(f\text{-}mppy)_2(dtbbpy)](PF_6)$ and $[Rh(dtbbpy)_3](PF_6)_3$ in the appropriate reaction media were distributed. A typical sample for the PS−WRC combination study contained 10 μmol of the PS and WRC catalysts in 10 mL of a 0.6 M TEOA solution in 90% ACN−water.

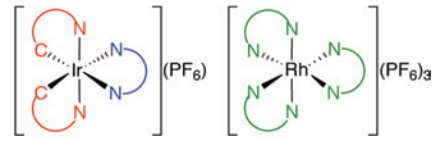

Figure 1. General structure of the Ir(III) PS and Rh(III) WRC used for the photochemical H_2-production studies (Figure 2 for C^N and N^N ligands).

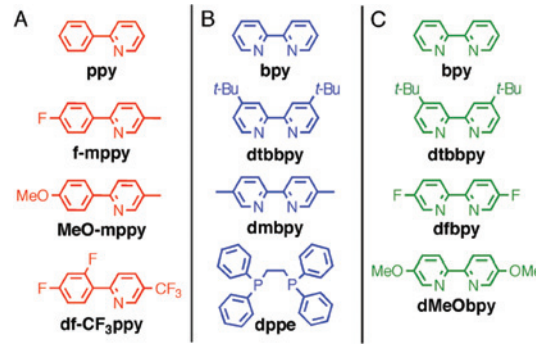

Figure 2. A) C^N ligands used for $[Ir(C^N)_2(bpy)]^+$ and $[Ir(C^N)_2(dtbbpy)]^+$ complexes; B) neutral ligands used for $[Ir(ppy)_2(N^N)]^+$ and $[Ir(ppy)_2(P^P)]^+$ complexes; C) N^N ligands used for $[Rh(N^N)_3]^{3+}$ complexes.

The photocatalytic reactions were evaluated in parallel fashion using a home-built 16-sample photoreactor with real-time analysis of gas evolution as described previously.[10] Samples were deoxygenated with six consecutive cycles of a 30 s gas evacuation followed by backfilling with an atmosphere of argon and then subjected to continuous photolysis with bottom illumination (460 nm, 500 ± 50 mW) until gas evolution ceased. Analysis of the reaction headspace by gas chromatography or a residual gas analyzer quantified hydrogen production. Detailed descriptions of the experiments and equipment are included in the Supporting Information.

Electrochemistry. Electrochemical experiments were conducted using a CH-Instruments Electrochemical Analyzer Model 600C potentiostat with a 1 mm^2 platinum disk working electrode, a coiled platinum wire supporting electrode, and a silver wire pseudoreference electrode. Ferrocene (Sigma) was employed as an internal reference, and measured potentials were later referenced to the standard calomel electrode (SCE). Solutions for voltammetric analysis were prepared in a 0.1 M solution tetra-*n*-butylammonium hexafluorophospate (TBAH) in acetonitrile (ACN). The experiments were conducted at approximately 1 mM concentration of the complex of interest at various scan rates ranging from 10 mV/s to 10 V/s.

Results and Discussion

Synthesis. $[Rh(bpy)_2Cl_2]^+$ is known to be kinetically inert, and the synthesis of $Rh(bpy)_3^{3+}$ requires either harsh forcing conditions for long time periods or the addition of a reducing agent.[27,28] Facile synthesis of the $[Rh(N^N)_3]^{3+}$ complexes (Figures 1 and 2) was accomplished by the reaction of the appropriate bpy ligand with $RhCl_3 \cdot 2H_2O$ in refluxing EtOH/H_2O for 15 min, followed by the addition of a reducing equivalent of hydrazine and subsequent refluxing for 1 h under aerobic conditions. This method has previously been described for the synthesis of $[Rh(bpy)_3]^{3+}$; however, the

(26) Sprouse, S.; King, K. A.; Spellane, P. J.; Watts, R. J. *J. Am. Chem. Soc.* **1984**, *106*, 6647–6653.
(27) Hillis, J. E.; DeArmond, M. K. *J. Lumin.* **1971**, *4*, 273–290.
(28) McKenzie, L. D.; Plowman, R. A. *J. Inorg. Nucl. Chem.* **1970**, *32*, 199–212.

specific attributes of the reaction have not been detailed.[27,29] Titration of the hydrazine equivalency (Supporting Information) indicates that under aerobic conditions the reaction is not catalytic, requiring a full equivalent of hydrazine to reduce $[Rh(bpy)_2Cl_2]^+$ and promote ligand labilization. Subsequent reoxidation of $[Rh(bpy)_2]^+$ by dissolved oxygen would promote association of the third bpy ligand to form $[Rh(bpy)_3]^{3+}$. This procedure allowed the efficient synthesis of three previously unreported $[Rh(N^N)_3]^{3+}$ species (N^N is dfbpy, dMeObpy, or dtbbpy) and has proven to be generally applicable and robust.

The novel ligand 5,5′-difluoro-2,2′-bipyridine was prepared in 80% yield by a nickel-catalyzed homocoupling and recrystalization from EtOH. $[Ir(C^N)_2(N^N)]^+$ and $[Ir(C^N)_2(P^P)]^+$ complexes (Figures 1 and 2) were synthesized by preparation of the *tetrakis*-(C^N)-μ-(dichloro)-diiridium(III) complexes with the appropriate cyclometalating ligand (C^N) followed by dimer cleavage with the neutral ligands (N^N or P^P).[24] The Ir(III) and Rh(III) complexes (Figures 1 and 2) were purified by column chromatography or recrystalization, as appropriate, and isolated as the PF_6^- salt.

Catalyst Evaluation Criteria. The photoreactions are evaluated using a number of criteria that provide insight into the activity of the system. End-point results such as H_2 produced and TON are a composite of both catalytic rate and catalyst stability, so they provide little utility when attempting to assess a system's efficiency and robustness. By monitoring gas evolution at 5 s intervals over the reaction time-course and normalizing the result with a headspace composition analysis at the end point, we get a very detailed picture of the reaction in a kinetic trace. The first derivative of the kinetic trace provides information about the catalytic rate and the catalyst decay for each reaction. Because the systems involve an induction period as the WRC is converted to the active catalytic state, the maximum catalytic rate is used as the relevent rate in kinetic analysis with the assumption that the catalysts are still at the initial concentrations.

The maximum catalytic rate can be converted to quantum yield (QY) (0.5 H_2 per photon absorbed) using the calculated photon flow and the molar absorptivity of the PS (Supporting Information). The QY calculations disregard any light absorption from the WRC because $[Rh(N^N)_3]^{3+}$ does not absorb light in the visible region (N^*N* = bpy or dtbbpy, $\epsilon_{460\ nm} < 1\ M^{-1}cm^{-1}$ in ACN). The actual structure of the WRC catalyst in solution is unknown and cannot be accounted for in QY calculations, therefore making them a minimum estimate of the actual value. However, the dilute nature of the reactions and high photon flow of the LED ensure sufficient irradiation to overcome spectral interference from weakly absorbing molecules.

Catalyst System Comparison. Initially, the utility of $[Co(bpy)_3]^{2+}$ and $[Rh(bpy)_3]^{3+}$ as the WRC was compared by evaluating them with an equivalent amount of

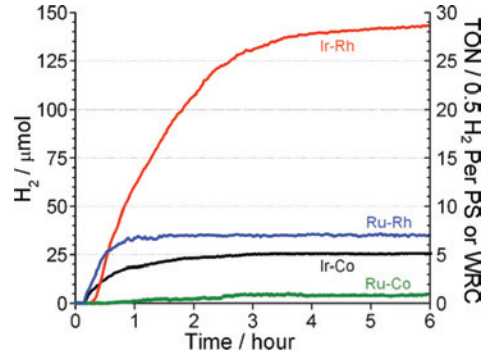

Figure 3. Evaluation of $[Ir(ppy)_2(bpy)](PF_6)$ or $[Ru(bpy)_3](PF_6)_2$ PS with $[Co(bpy)_3]Cl_2$ or $[Rh(dtbbpy)_3](PF_6)_3$ WRC in photosynthetic-H_2 reactions (10 μmol of PS and WRC, 10 mL of 0.6 M TEOA in 50% ACN-H_2O, 460 nm, 500 mW, 18 h).

$[Ru(bpy)_3]^{2+}$ or $[Ir(ppy)_2(bpy)]^+$ PS in a photosynthetic reaction with 0.6 M TEOA in 50% ACN-H_2O. The reaction kinetic trace in Figure 3 shows that $[Ir(ppy)_2(bpy)]^+$ outperforms $[Ru(bpy)_3]^{2+}$ when evaluated with either WRC. When evaluated with the Ir−PS, $[Rh(bpy)_3]^{3+}$ was much more active with a maximum catalytic rate of 23 turnovers per hour (TOF, 0.5 H_2 per catalyst per hour) and overall efficiency of 29 TON compared to 9.5 TOF (h^{-1}) and 5 TON for $[Co(bpy)_3]^{2+}$ (Supporting Information). Both H_2-evolution kinetics plots can be fitted with a unimolecular exponential decay function, as described in ref 10, which indicates that the activity of the Co(II) system is decaying at nearly twice the rate of the more robust Rh(III) system (Supporting Information).

Structure−Activity Relationships. The promising preliminary results for the Ir−Rh system warranted further investigation but the complicated nature of multicomponent photocatalytic systems makes the improvement of such systems through the study of their physical properties a nearly impossible task. To make rapid improvements, synthetic modification was used to develop a group of catalysts with molecular diversity. The heteroleptic Ir(III) PSs are perfectly suited for synthetic tuning because ligand substitutions on the cyclometalating and neutral ligands allow the energy of the highest occupied and lowest unoccupied molecular orbitals to be modified independently. Seven diverse PSs with a range of photophysical and electrochemical properties were prepared (Figures 1 and 2).[13,18,24,30] The Rh WRCs had not been studied previously, so four diverse bpys were chosen to determine the effect of electron withdrawing and donating substituents on catalyst activity (Figures 1 and 2). The seven Ir PSs and four Rh WRCs were evaluated in a 0.6 M TEOA solution with 90% ACN−H_2O, for which studies indicated was the optimal ACN−H_2O mixture for the Ir−Rh system (Supporting Information). The end-point results, presented in Figure 4, indicate that dtbbpy is the optimal N^N ligand for both PS and WRC, whereas the f-mppy and MeO-mppy cyclometallating ligands are equally effective.

To confirm the previous results and determine which cyclometalating ligand outperforms the rest, all four C^N ligands were evaluated with the optimal N^N ligand, dtbbpy.

(29) Gillard, R. D.; Heaton, B. T. *Coor. Chem. Rev.* **1972**, *8*, 149–157.

(30) Lowry, M. S.; Bernhard, S. *Chem.—Eur. J.* **2006**, *12*, 7970–7977.

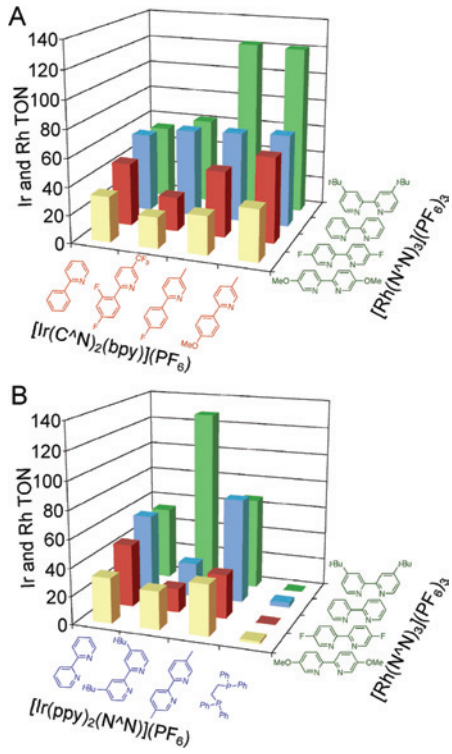

Figure 4. Evaluation of $[Ir(C^N)_2(N^N)](PF_6)$ and $[Rh(N^N)_3](PF_6)_3$ in photosynthetic-H_2 reactions (1 μmol of PS and WRC in 10 mL of 0.6 M sol of SR in 90% Solvent-H_2O, 460 nm, 500 mW, 20−24 h) with the SR and solvent indicated in the graph.

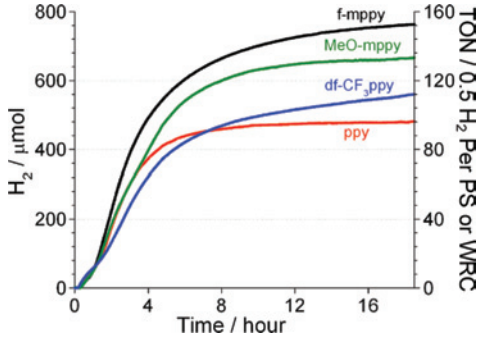

Figure 5. Evaluation of $[Ir(C^N)_2(dtbbpy)](PF_6)$ and $[Rh(dtbbpy)_3](PF_6)_3$ in photosynthetic-H_2 reactions (10 μmol of PS and WRC in 10 mL of 0.6 M sol of TEOA in 90% ACN−H_2O, 460 nm, 500 mW, 18 h).

The kinetic traces in Figure 5 indicate that the combination of $[Ir(f\text{-}mppy)_2(dtbbpy)]^+$ and $[Rh(dtbbpy)_3]^{3+}$ is the most effective catalyst system under the conditions employed with more than 150 TON and a maximum rate of 39 TOF (h^{-1}) for a QY of 11.5%. The use of synthetic modification and catalyst screening allowed for a rapid improvement in catalytic activity and efficiency, further validating our screening approach. All of the subsequent studies were conducted using the optimal PS-WRC combination of $[Ir(f\text{-}mppy)_2(dtbbpy)]^+$ and $[Rh(dtbbpy)_3]^{3+}$ described above.

Photoreaction Condition Optimization. Reaction conditions such as sacrificial reductant, solvent environment, and catalyst concentration have a dramatic effect on the performance of artificial photosynthetic systems. Following the completion of the SAR study, we optimized the reaction

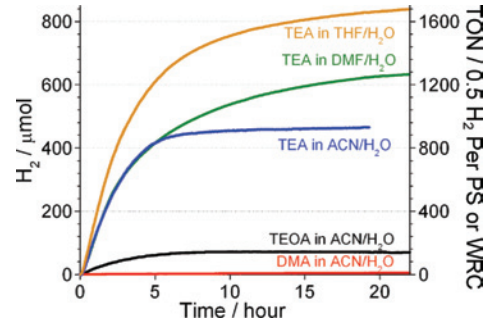

Figure 6. Evaluation of $[Ir(f\text{-}mppy)_2(dtbbpy)](PF_6)$ and $[Rh(dtbbpy)_3](PF_6)_3$ in photosynthetic-H_2 reactions (1 μmol of PS and WRC in 10 mL of 0.6 M sol of SR in 90% solvent-H_2O, 460 nm, 500 mW, 20−24 h) with the SR and solvent indicated in the graph.

conditions to achieve the highest possible catalytic activity while exploring the properties and limitations of the Ir−Rh system.

A. Sacrificial Reductant. The SR can play a large role in the activity of the catalytic system because it affects the properties of the reaction medium (pH, dielectric constant, solvent viscosity), which can influence the observed rates of the various electron transfers and metal-hydride formation. In the Ir−Rh system, the SR has an even greater influence than in traditional ruthenium-based systems because the Ir−Rh system functions through a reductive quenching mechanism (below) that depends on efficient quenching of the excited-state PS by the SR.

DMA and TEA are two SRs that have been previously utilized in photocatalytic water-reduction systems.[23,31,32] Using laser flash photolysis to measure dynamic quenching (Supporting Information), the quenching constants for DMA ($k_q = 5.6 \times 10^9\ M^{-1}s^{-1}$) and TEA ($k_q = 1.2 \times 10^8\ M^{-1}s^{-1}$) were determined for $[Ir(ppy)_2(bpy)]^+$ and compared to the literature value for TEOA ($k_q = 5.4 \times 10^6\ M^{-1}s^{-1}$). We evaluated the use of these two amines as the SR with the optimal PS−WRC combination, and the kinetic traces in Figure 6 show that the aliphatic amine TEA gives a dramatic increase in catalytic rate and a 6-fold increase in total hydrogen production compared to TEOA. Counter-intuitively, the system using the DMA, the best quencher of the three SRs studied, exhibited little catalytic activity compared to the aliphatic amines TEOA or TEA. This result may indicate that for DMA quenching involves energy-transfer rather than electron-transfer quenching, that charge recombination is occurring, or that DMA creates an unfavorable environment for the WRC−hydride formation. All subsequent studies were conducted using TEA as the SR.

B. Solvent Environment. In homogeneous catalysis, the solvent environment often plays a critical role in the activity and stability of the catalysts. The electrostatic properties of the medium can affect the photophysical properties of the PS as well as the Coulombic interactions and the rates of ET between the PS and WRC components.[33,34] Additionally, the ligating ability of the solvent may influence the reaction by stabilizing or destabilizing key redox intermediates.[32]

(31) DeLaive, P. J.; Sullivan, B. P.; Meyer, T. J.; Whitten, D. G. *J. Am. Chem. Soc.* **1979**, *101*, 4007–4008.

Table 1. Results for [Ir(f-mppy)2(dtbbpy)](PF_6) and [Rh(dtbbpy)$_3$](PF_6)$_3$ in Photosynthetic-H_2 Reactions the Optimal Solvent Ratio (1 μmol of PS and WRC in 10 mL of 0.6 M TEA in THF−H_2O, 460 nm, 500 mW, 18 h)

THF−H_2O (%)	H_2 (μmol)	TON	max rate (μmol/h)
50	423	846	127
70	732	1463	173
75	918	1835	180
80	1063	2126	182
85	934	1868	173
90	840	1680	203
95	625	1251	153
99.9	360	721	86

Previous studies of the Ir−PS using mass spectrometry showed that ACN displacement of the bipyridine ligand accompanied the observed decay in catalyst activity.[10] In an effort to improve the catalyst activity and stability in the Ir−Rh system, additional solvents with less coordinating strength than ACN were tested with the optimal PS−WRC combination in 0.6 M TEA with a 9:1 solvent−water mixture. Improved results were achieved with both DMF and THF, whose reaction kinetic traces are presented in Figure 6. Both solvents are much weaker ligands than ACN, whereas calculations of the static dielectric constant using the Kirkwood theory for multicomponent mixtures reveals that the ACN and DMF mixtures have very similar values, whereas the THF mixture will be much lower.[35] The results show that the ACN and DMF reactions have identical catalytic rates during the intial five hours, yet in DMF the catalysts show greater stability allowing it to outperform the ACN reaction over the extended reaction period. The THF reaction shows the same improvement of catalyst stability with the expected increase in catalytic rate due to its lower dielectric constant.

The early studies for catalyst system comparison were conducted in a 0.6 M TEOA solution using a 1:1 mixture of ACN and water. A study evaluating solvent ratio (Supporting Information) showed that catalyst performance improves at higher ACN concentrations, with maximum H_2-production in 9:1 ACN−water. This phenomenon could be attributed to a balance between the benefit of the lower dielectric constant at high ACN concentration with the need for water as a proton source for Rh-hydride formation.[36] To determine the optimal solvent ratio for the TEA−THF−water system, eight different compositions ranging from 1:1 to 1000:1 THF-water were evaluated with the optimal PS−WRC combination. The results in Table 1 show that, although the highest catalytic rates were achieved in 90% THF−water, the 80% THF system was more productive over the course of the reaction and the optimized ratio of THF−water was used for all subsequent studies.

C. Isotope Labeling. The results in Table 1 indicate that with less than 0.1% water available the photocatalytic system continues to function. To ensure that the hydrogen production is not the result of the direct dehydrogenation of TEA, isotope labeling experiments were conducted. The optimal PS−WRC combination using 0.6 M TEA in 8:2 THF−D_2O resulted in a gas composition of 2:12:86 H_2:HD:D_2 for 92% deuterium incorporation. A similar experiment using an 8:1:1 mixture of THF−H_2O−D_2O showed little difference in the rate of gas evolution but the gas composition was 70:27:3 H_2:HD:D_2 for only 17% deuterium incorporation. Thus, although there is an obvious kinetic isotope effect involving the formation of the rhodium hydride species, this is not the rate-limiting step in the photosynthetic reactions and the overall rate of H_2 production is unaffected. This isotope effect explains the 8% hydrogen that is incorporated in the gas mixture for the 8:2 THF−D_2O reaction because the small amount of protons generated in the SR oxidation and decomposition (below) will be selectively reduced over the available deuterium for a disproportionate representation in the final product. The isotope labeling clearly demonstrates that our system selectively reduces water to produce hydrogen.

D. Catalyst Concentration. As substantial increases in catalyst activity were achieved, catalyst loading was reduced so that the reactions would operate within the capacity of the photoreactor setup. From preliminary results, a marked increase in efficiency and catalytic activity was noticed as the systems approached lower catalyst concentrations. This result is counter-intuitive because outer-sphere ET processes should be more efficient at higher concentration. Additionally, the PS concentrations in the photoreactions are sufficiently low to ensure that the reactions are not light-limited. This indicates that competitive deactivation pathways are prevalent at higher concentrations, such as the self-annihilation between rhodium hydride and $[Rh(bpy)_3]^{3+}$ noted previously in studies of the radiolytic reduction of water.[37]

To examine the concentration dependence more thoroughly, an experiment was conducted varying PS and WRC concentrations independently in the range of 0.05 to 0.15 M. The results of this 25-reaction array (Figure 7) demonstrate that catalyst performance improves when one component is evaluated with an excess of the other component, and more than 5000 TON are achieved for either the PS or the WRC. The use of an equivalent amount of PS and WRC balances the performance of both components. Looking at the PS and WRC TON for the series of 1:1 PS-WRC reactions (parts A and B of Figure 7), the catalysts have a maximum efficiency around 0.1 mM concentration. The combination of QY, catalytic rates and TON are optimized at 0.075 mM PS and WRC concentration. This results in 3400 TON and a maximum catalytic rate of 520 TOF (h^{-1}), which equates to a QY of 32% (part C of Figure 7). This marks more than two orders of magnitude improvement over the original Ir−Rh system (Figure 3).

Reaction Mechanism. The photocatalytic water reduction process reported above involves three critical components: the PS, the SR, and WRC. In the catalytic light cycle, the PS is responsible for the absorption of visible light to provide

(32) Ziessel, R.; Hawecker, J.; Lehn, J. *Helv. Chim. Acta* **1986**, *69*, 1065–1084.
(33) Brunschwig, B. S.; Ehrenson, S.; Sutin, N. *J. Phys. Chem.* **1987**, *91*, 4714–4723.
(34) Borchardt, D.; Wherland, S. *Inorg. Chem.* **1984**, *23*, 2537–2542.
(35) Wang, P.; Anderko, A. *Fluid Phase Equilib.* **2001**, *186*, 103–122.
(36) Bakac, A. *J. Chem. Soc., Dalton Trans.* **2006**, 1589–1596.
(37) Mulazzani, Q. G.; Venturi, M.; Hoffman, M. Z. *J. Phys. Chem.* **1982**, *86*, 242–247.

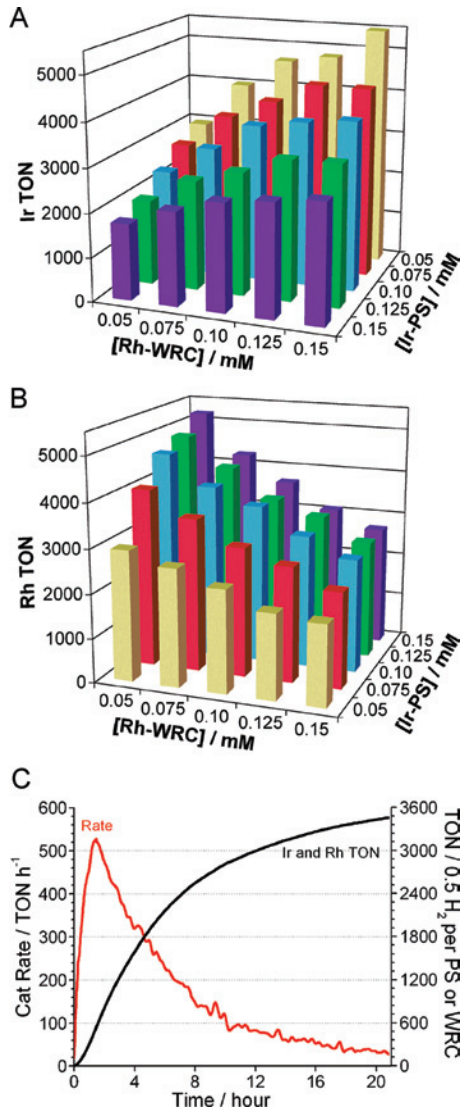

Figure 7. A) Ir TON, B) Rh TON, and C) kinetic and rate trace (at 0.075 mM PS and WRC) from a study evaluating the effect of catalyst concentration on performance with $[Ir(f\text{-}mppy)_2(dtbbpy)](PF_6)$ and $[Rh(dtbbpy)_3](PF_6)_3$ in photosynthetic-H_2 reactions (0.5−1.5 μmol of PS and WRC in 10 mL of 0.6 M TEA in 80% THF−H_2O, 460 nm, 500 mW, 22 h).

the energy necessary for the endothermic water reduction process to occur. In the catalytic dark cycle, the WRC collects the high-energy electrons from the light cycle and protons from water to produce hydrogen. The SR provides the electrons necessary for water reduction by replenishing the lowest singly occupied molecular orbital of the PS* or PS^+, depending on the mechanism of quenching. The interactions of all three components and their corresponding redox intermediates determine the mechanism and energetics of the process. Photophysical and electrochemical characterization of the components provides insight into the nature of these interactions in the optimized system.

A. Sacrificial Reductant. Aliphatic tertiary amines have traditionally been employed as the SR in photocatalytic systems for water reduction, and their oxidation and subsequent degradation (eqs 1−4) have been studied previously.[38−40] The oxidation peak potential for TEA at pH 12 in water is reported to be 0.69 V (vs SCE).[41] Following the initial one-electron oxidation, the TEA^+ radical cation is rapidly deprotonated and undergoes a radical shift to the α-carbon. This neutral carbon radical species is expected to be highly reducing, and a second oxidation forms the iminium cation, which is hydrolyzed to form DEA and acetaldehyde. Thus, each TEA is capable of donating two electrons and two protons. Rapid conversion of the oxidized TEA species, as outlined in eqs 2 and 4, avoid any possible back reactions between the oxidized TEA species and the reduced PS or WRC species.

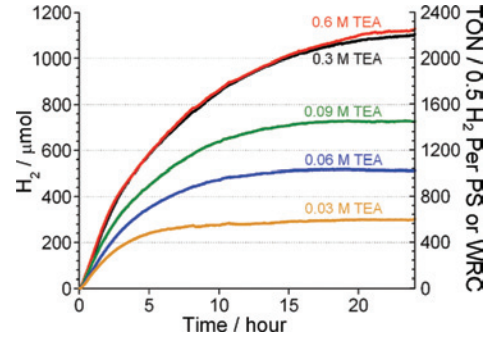

Figure 8. Evaluation of $[Ir(f\text{-}mppy)_2(dtbbpy)](PF_6)$ and $[Rh(dtbbpy)_3](PF_6)_3$ in photosynthetic-H_2 reactions (1 μmol of PS and WRC in 10 mL of 80% THF−H_2O, 460 nm, 500 mW, 20−24 h) with varying TEA concentrations.

$$TEA \rightarrow Et_2\overset{\bullet+}{N}CH_2CH_3 + e^- \quad (1)$$

$$Et_2\overset{\bullet+}{N}CH_2CH_3 \rightarrow Et_2N\dot{C}HCH_3 + H^+ \quad (2)$$

$$Et_2N\dot{C}HCH_3 \rightarrow Et_2\overset{+}{N}{=}CHCH_3 + e^- \quad (3)$$

$$Et_2\overset{+}{N}{=}CHCH_3 \rightarrow DEA + CH_3CHO + H^+ \quad (4)$$

During the course of the photoreaction, the pH and solvent composition may gradually change as a result of the degradation of TEA or the reduction of water, potentially leading to a substantial change in reaction conditions when the system achieves high TON. As proven by the isotope experiment, the protons from water are reduced in the dark cycle to produce hydrogen, yet these protons are replenished during the dielectronic reduction and degradation of TEA. Thus, the net change in reaction condition is the partial conversion of TEA to DEA, which have similar pK_a values, and the consumption of 1−2% of the water. To ensure that sufficient TEA is still available at all time points in the reaction, the dependency on TEA concentration was studied. The kinetic traces in Figure 8 indicate that the catalytic rate and overall reaction are not affected at concentrations as low as 0.3 M TEA. In the current investigations, we can be certain that any decrease in activity at later time points during the

(38) Ross, S. D. *Tetrahedron Lett.* **1973**, *14*, 1237–1240.
(39) Cohen, S. G.; Parola, A.; Parsons, G. H. *Chem. Rev.* **1973**, *73*, 141–161.
(40) DeLaive, P. J.; Foreman, T. K.; Giannotti, C.; Whitten, D. G. *J. Am. Chem. Soc.* **1980**, *102*, 5627–5631.
(41) Chow, Y. L.; Danen, W. C.; Nelsen, S. F.; Rosenblatt, D. H. *Chem. Rev.* **1978**, *78*, 243–274.

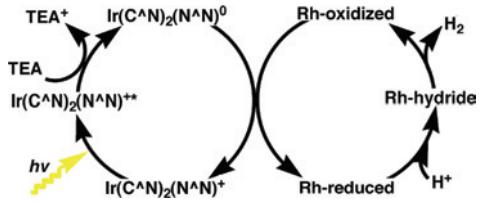

Figure 9. General reaction scheme for photocatalytic hydrogen production by TEA−Ir−Rh system.

photoreactions are due to catalyst degradation instead of changes in the reaction environment.

B. Light Cycle. The central component of the catalytic system drives photosynthesis through charge transfer of a high-energy electron to the dark-cycle catalytic components. Following visible-light excitation (460 nm, $\epsilon = 553 \pm 5\ M^{-1}cm^{-1}$ in 80% THF/H_2O), $[Ir(f\text{-}mppy)_2(dtbbpy)](PF_6)$ achieves a long-lived charge-separated state (eq 5) with a 1.15 μs decay lifetime similar to that seen for the classical PS $[Ru(bpy)_3](PF_6)_2$. The excited-state is then quenched through two different pathways: reductive quenching by the SR (eq 6) or oxidative quenching by the components of the dark cycle (eq 7). Laser flash photolysis and Stern−Volmer analyses (Supporting Information) yielded the quenching constants for the optimal system. The rate constants for reductive quenching of $[Ir(f\text{-}mppy)_2(dtbbpy)]^{+*}$ by TEA and oxidative quenching by $[Rh(dtbbpy)_3]^{3+}$ are roughly equivalent ($k_{ox} = 6.7 \times 10^7\ M^{-1}s^{-1}$ and $k_{red} = 6.4 \times 10^7\ M^{-1}s^{-1}$). Because TEA is present at more than 1000 times the concentration of $[Rh(dtbbpy)_3]^{3+}$, the reaction is operating predominately through a reductive quenching mechanism, where the highly reactive $[Ir(f\text{-}mppy)_2(dtbbpy)]^0$ species reduces the WRC components as outlined in Figure 9.

$$PS \xrightarrow{h\nu} PS^* \tag{5}$$

$$PS^* + TEA \xrightarrow{K_{red}} PS^- + TEA^+ \tag{6}$$

$$PS^* + Rh(N^{\wedge}N)_3^{3+} \xrightarrow{K_{ox}} PS^+ + Rh(N^{\wedge}N)_3^{2+} \tag{7}$$

The reaction pathway has a major effect on the reaction energetics because the reducing equivalents available to the WRC come from the reduced or excited PS for the reductive or oxidative quenching pathways, respectively. Cyclometallated Ir(III) complexes are distinct from traditional Ru(II) PSs in that the excited-state species, $[Ir(ppy)_2(bpy)]^{+*}$, can be reductively quenched by tertiary amines. The electrochemical and emission data for many of the compounds evaluated in this study were previously reported.[13,18] With the ground-state oxidation potential and the triplet-singlet relaxation energy, a minimal estimate of the excited-state oxidation potential can be made using Hess' Law. $[Ir(f\text{-}mppy)_2(dtbbpy)](PF_6)$ has a reversible one-electron reduction potential of $E^{\circ\prime} = -1.50$ V ($\Delta E_p = 67$ mV, vs SCE) and an excited-state oxidation potential of $E^{\circ\prime} = -0.94$ V (vs SCE). The corresponding excited-state oxidation potential for $[Ru(bpy)_3](PF_6)_2$, the only reducing equivalent available for the classic Ru-PS, is $E^{\circ\prime} = -0.78$ V (vs SCE). Reductive quenching of the excited Ir−PS by the SR yields much higher energy reducing equivalents than oxidative quenching by the WRC.

C. Dark Cycle. Published electrochemical studies of $[Rh(bpy)_3](PF_6)_3$ and related complexes in ACN have demonstrated complex electrochemical behavior attributed to an irreversible ECEC mechanism.[42,43] The cyclic voltammogram of $[Rh(dtbbpy)_3](PF_6)_3$ (part B of Figure 10) shows very similar electrochemistry to that of the unsubstituted form (part A of Figure 10). The increased electron donation of the *tert*-butyl substitutions on the bpy ligands results in a negative shift of all of the reduction peaks as expected. Cathodic waves I and II correspond to irreversible one-electron reductions ($E_{pa} = -0.96$ V and $E_{pa} = -1.15$ V vs SCE at 100 mV/s) that are accompanied by ligand labilization to form $[Rh(dtbbpy)_2]^+$. Parts C−F of Figure 10 show that reversing the scans immediately following waves I or II imparts some reversibility at high scan rates as expected with an EC mechanism. The reversible cathodic wave III represents the formation of $[Rh(dtbbpy)_2]^0$ ($E^{\circ\prime} = -1.45$ V vs SCE, $\Delta E = 66$ mV).

$$PS^- + Rh(N^{\wedge}N)_3^{3+} \rightarrow PS + Rh(N^{\wedge}N)_3^{2+} \tag{8}$$

$$Rh(N^{\wedge}N)_3^{2+} \rightarrow Rh(N^{\wedge}N)_2^{2+} + N^{\wedge}N \tag{9}$$

$$PS^- + Rh(N^{\wedge}N)_2^{2+} \rightarrow PS + Rh(N^{\wedge}N)_2^{+} \tag{10}$$

$$PS^- + Rh(N^{\wedge}N)_2^{+} \rightarrow PS + Rh(N^{\wedge}N)_2^{0} \tag{11}$$

The active catalytic state of the WRC component is unknown, although the Ir−Rh system exhibits an induction period up to 1 h before it reaches maximum activity, as illustrated in the part C of Figure 7, indicating the conversion of the WRC to a different species as the active catalyst. The electrochemical data indicates that $[Rh(N^{\wedge}N)_3]^{3+}$ will initially form $[Rh(N^{\wedge}N)_2]^+$ following two consecutive reductions and ligand labilization (eqs 8−10). This was confirmed by a comparison of $[Rh(N^{\wedge}N)_3]^{3+}$ and $[Rh(N^{\wedge}N)_2Cl_2]^+$ (Supporting Information) that showed no difference in catalytic activity between the tris- and bis-bipyridyl Rh(III) species. Although earlier publications postulated that $[Rh(N^{\wedge}N)_2]^+$ is the active catalyst species,[5] it has been noted that the Rh(I) species is stable in both acidic and alkaline solution for months.[44] Mulazanni and co-workers hypothesized that the Rh(III)-hydride could form and then be further reduced to form a Rh(II)-hydride as the direct precursor to H_2,[37] similar to the mechanism proposed for Rh-porphyrins.[45] The high-energy reducing equivalents from the reductive quenching mechanism provides the necessary energy for the $[Rh(N^{\wedge}N)_2]^+$ species to be reduced to form $[Rh(N^{\wedge}N)_2]^0$ per eq 11. This species would then form a Rh(II) hydride, which

(42) Kew, G.; DeArmond, K.; Hanck, K. *J. Phys. Chem.* **1974**, *78*, 727–734.
(43) Creutz, C.; Keller, A. D.; Sutin, N.; Zipp, A. P. *J. Am. Chem. Soc.* **1982**, *104*, 3618–3627.
(44) Mulazzani, Q. G.; Emmi, S.; Hoffman, M. Z.; Venturi, M. *J. Am. Chem. Soc.* **1981**, *103*, 3362–3370.
(45) Grass, V.; Lexa, D.; Saveant, J. *J. Am. Chem. Soc.* **1997**, *119*, 7526–7532.

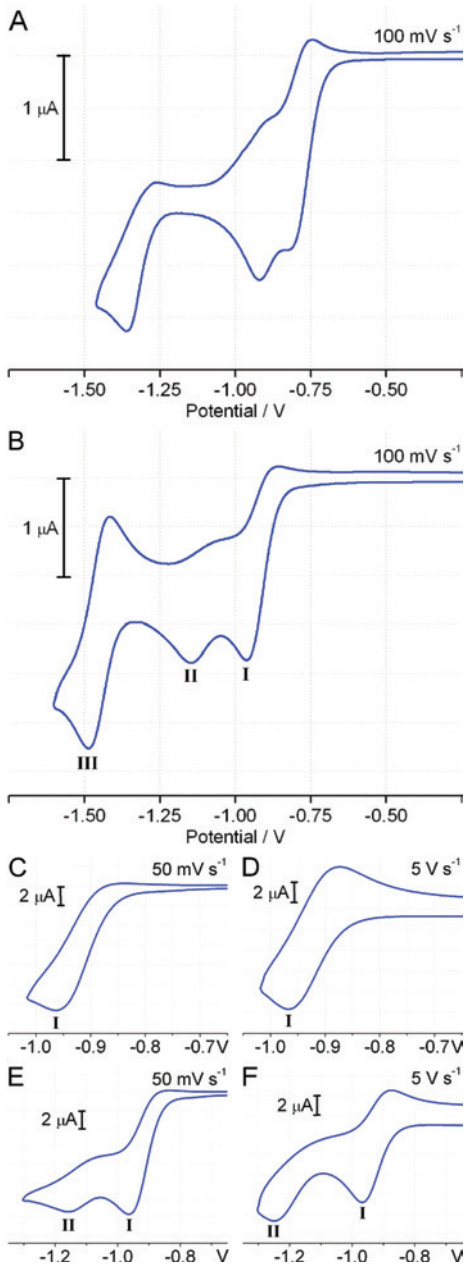

Figure 10. Cyclic voltammograms of $[Rh(bpy)_3](PF_6)_3$ (Inset A) and $[Rh(dtbbpy)_3](PF_6)_3$ (Insets B−F), 0.5 mM concentration in ACN with 0.1 M TBAH, 1 mm^2 platinum disk working electrode, a coiled platinum wire supporting electrode, silver wire pseudoreference electrode using ferrocene as an internal standard referenced at 0.37 V vs SCE.

could produce hydrogen in a homolytic bimolecular pathway or form a rhodium dihydride that produces hydrogen by reductive elimination in a homolytic unimolecular pathway.

Homogeneous or Heterogeneous Catalysis. In any homogeneous system where reducing conditions exist, care must be taken to ensure that the catalytic activity originates from an actual molecular species and not a colloidal metal formed through catalyst decomposition. It has recently been proven in two separate instances that Pt(II) or Pd(II) molecular catalysts were actually decomposing to form colloids, which were the active catalyst species.[46,47] The reaction kinetics for the Ir−Rh system reveal an induction period and sigmoidal kinetics (part C of Figure 7), which are often viewed as strong evidence of slow formation of a highly active colloidal species followed by deactivation as the nanoparticles agglomerate to form inactive bulk metal.[48] However, the kinetics could also be attributed to the electrochemical transformation of the precatalyst to form the active catalytic species, as outlined in eqs 8−11, followed by the degradation of the PS as observed previously.[10] There is no single definitive experiment to make the distinction between homogeneous and heterogeneous catalysis and a variety of methods must be used to reach a convincing conclusion regarding the actual catalytic mechanism.[49]

A. Rhodium Colloids. Colloidal rhodium has been used in the photochemical production of hydrogen in at least one instance, although it was less active than the standard platinum colloid and did not seem to be a promising candidate.[8] If $[Rh(N^{\wedge}N)_3]^{3+}$ was a precursor for colloid formation, the activity of all species would be expected to be similar, so the SAR for the different ligand substitutions (Figure 4) seems to indicate a true homogeneous catalyst. It cannot be ruled out, however, that the different N^N ligands would not have an effect on colloid formation if the reaction were occurring through a heterogeneous mechanism.

To evaluate the activity of rhodium colloids in the present system, several attempts were made to prepare colloid samples for comparison (Supporting Information). Tertiary amines are known to stabilize rhodium colloids,[50] so it is feasible that colloid formation might be favored under the reaction conditions employed in the present studies. An experiment substituting $RhCl_3 \cdot 2H_2O$ as a potential colloid precursor shows little catalytic activity when compared to $[Rh(dtbbpy)_3](PF_6)_3$. Attempts to presynthesize colloids by the conditions employed in ref 50 resulted in the formation of large particulate rhodium that showed no activity in the Ir−Rh system. Additionally, a polymer-protected rhodium colloid was synthesized according to literature procedure,[51] for use as a positive control in the poisoning tests described below, yet it too showed negligible catalytic activity in our system.

B. Mercury Poisoning. The ability of mercury to poison nanoparticulate metal catalysts is a widely used test to establish reaction mechanism, and the discovery of platinum colloid formation in a supposed homogeneous system using this method was recently reported.[47] The rhodium amalgam is known to form, albeit with more difficulty than the platinum amalgam,[52] and mercury poisoning has been reported for rhodium colloids.[48,53] To test the Ir−Rh system, the pristine reaction was compared to both a reaction pretreated with mercury then filtered prior to illumination and a reaction treated with mercury during illumination. If catalytic activity is the result of rhodium colloids forming from degradation of the precatalyst during the photoreaction, then pretreatment with mercury should not affect catalytic

(46) Lei, P.; Hedlund, M.; Lomoth, R.; Rensmo, H.; Johansson, O.; Hammarstrom, L. *J. Am. Chem. Soc.* **2008**, *130*, 26–27.
(47) Du, P.; Schneider, J.; Li, F.; Zhao, W.; Patel, U.; Castellano, F. N.; Eisenberg, R. *J. Am. Chem. Soc.* **2008**, *130*, 5056–5058.
(48) Weddle, K.; Aiken, J.; Finke, R. *J. Am. Chem. Soc.* **1998**, *120*, 5653–5666.

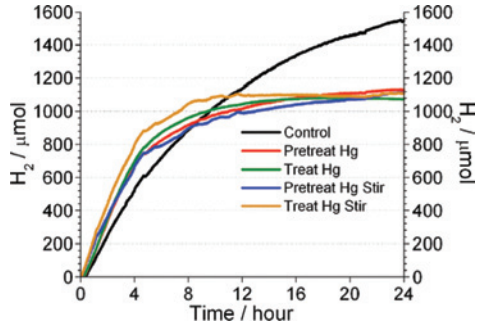

Figure 11. $[Ir(f\text{-}mppy)_2(dtbbpy)](PF_6)$ with $[Rh(dtbbpy)_3](PF_6)_3$ in photosynthetic-H_2 reactions (0.5 μmol of PS and WRC in 10 mL of 0.6 M sol of TEA in 80% THF−H_2O, 460 nm, 500 mW, 24 h) that are untreated, pretreated with Hg (1 g) for 1 h then filtered, or treated with Hg (1 g) during illumination; shaking 150 rpm or stirring 1200 rpm.

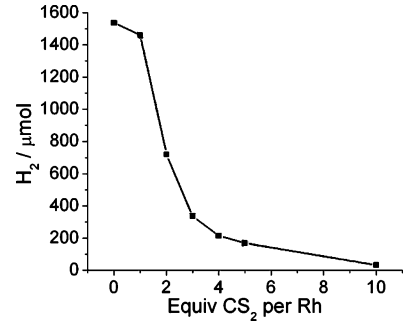

Figure 12. End-point results for quantitative poisoning of $[Ir(f\text{-}mppy)_2(dtbbpy)](PF_6)$ with $[Rh(dtbbpy)_3](PF_6)_3$ in photosynthetic-H_2 reactions (0.5 μmol of PS and WRC in 10 mL of 0.6 M sol of TEA in 80% THF−H_2O, 460 nm, 500 mW, 24 h) with CS_2 (0, 0.5, 1, 1.5, 2, 2.5, or 5 μmol).

activity and the addition of mercury during illumination should poison the system such that little or no activity is observed.

The results of the mercury test, presented in Figure 11, showed a similar effect for both the pretreated and treated systems with increased initial rates and shorter system lifetimes. The majority of the catalytic activity is retained in the mercury test, indicating that the catalytic activity is not due to rhodium colloid formation and that any effect is due to an unknown interaction between mercury and the solvent, SR, PS, or WRC, irrespective of the photoreaction itself. Finke and co-workers highlighted the need for a large excess of mercury (at least 300 equiv) and good stirring to ensure that a lack of catalyst poisoning is in fact due to the absence of a colloid.[49] The present study utilized more than 10 000 equiv of mercury, and vigorous stirring of the mercury test photoreactions at 1200 rpm showed not significant difference to orbital shaking at 150 rpm ensuring that the test is not mass transfer limited. Without a catalytically active rhodium colloid sample for comparison as a positive control, however, we cannot be absolutely certain that the lack of poisoning indicates a true homogeneous system.

C. Quantitative CS_2 Poisoning. Quantitative poisoning studies can discern whether a system operates by heterogeneous or homogeneous catalysis using ligands that bind strongly to metal centers and have the ability to poison both heterogeneous and molecular species.[49] A heterogeneous species will have only a fraction of the metal atoms on the surface and will be poisoned completely with $\ll$1 equiv of the poison ligand, while a molecular catalyst will require $\geqslant$1 equiv for complete poisoning. For example, CS_2 has been shown to poison most of the catalytic activity of rhodium nanoclusters used for cyclohexene hydrogenation with less than 0.018 equiv of CS_2 per rhodium.[54] For the Ir−Rh system, the addition of CS_2 to the photoreactions required multiple equivalents of CS_2 to poison catalyst activity (Figure 12), as would be expected for a homogeneous system. The effect of CS_2 poisoning shows increased poisoning at 2 and 3 equiv with only 10% of activity remaining at 5 equiv of CS_2. The activity slowly approaches zero at higher concentrations, and it appears that competitive binding between dtbbpy and CS_2 occurs. These results reinforce the mercury poison test and provide strong evidence that the Ir−Rh system does operate through a true homogeneous mechanism.

Conclusion

We have reported an efficient homogeneous catalytic system for the visible-light-induced production of hydrogen from water utilizing tris-2,2′-bipyridyl Rh(III) complexes. The synthetic modification and catalyst screening identified an optimal catalyst combination of $[Ir(f\text{-}mppy)_2(dtbbpy)](PF_6)$ and $[Rh(dtbbpy)_3](PF_6)_3$, and the systematic optimization of the reaction conditions led to more than 2 orders of magnitude improvement over the original system. We currently achieve more than 5000 TON for the PS and WRC with QYs greater than 34%. Photophysical and electrochemical characterization reveals that the reductive quenching pathway provides the necessary driving force to efficiently reduce water using the Rh−WRC. Mercury and quantitative CS_2 poison tests both provide strong evidence of a true molecular catalyst, and we are confident that the catalyst activity is the result of a homogeneous catalytic species. To the best of our knowledge, the results are superior to any other homogeneous photocatalytic system for water reduction.

Ongoing investigations of the complex mechanistic details of the Ir−Rh systems will aid the design of more robust catalysts. Additionally, we are working to incorporate the Ir−PS and Rh−WRC components into supramolecular water reduction systems for improved efficiency using a series of tailored bridging ligands.[55] Future work will attempt to develop complete water splitting systems using the system described herein and an iridium-based water oxidation catalyst.[56]

(49) Widegren, J. A.; Finke, R. G. *J. Mol. Catal. A: Chem.* **2003**, *198*, 317–341.
(50) Yonezawa, T.; Tominaga, T.; Richard, D. *J. Chem. Soc., Dalton Trans.* **1996**, 783–789.
(51) Wang, Q.; Liu, H.; Han, M.; Li, X.; Jiang, D. *J. Mol. Catal. A: Chem.* **1997**, *118*, 145–151.
(52) Guminski, C. *J. Mater. Sci.* **1989**, *24*, 3285–3288.
(53) Jaska, C. A.; Manners, I. *J. Am. Chem. Soc.* **2004**, *126*, 9776–9785.
(54) Hornstein, B.; Aiken, J.; Finke, R. *Inorg. Chem.* **2002**, *41*, 1625–1638.
(55) Bernhard, S.; Belser, P. *Synthesis* **1996**, *2*, 192–194.
(56) McDaniel, N.; Coughlin, F.; Tinker, L.; Bernhard, S. *J. Am. Chem. Soc.* **2008**, *130*, 210–217.

Acknowledgment. We thank Emily Barton, Neal McDaniel, and Lenny Tinker for their useful discussions. We thank Radhika Vemula for her assistance in the work. S.B. acknowledges support through a NSF CAREER award (CHE-0449755).

Supporting Information Available: Experimental notes and characterization for all ligands and complexes. Detailed experimental notes and additional results from photoreactions and dynamic quenching studies. An efficient homogeneous catalytic system for the visible-light-induced production of hydrogen from water utilizing cyclometalated iridium(III) and tris-2,2′-bipyridyl rhodium(III) complexes is described. Synthetic modification of the photosensitizer $Ir(C\hat{}N)_2(N\hat{}N)^+$ and water reduction catalyst $Rh(N\hat{}N)_3^{3+}$ creates a family of catalysts with diverse properties. Parallel screening of the various catalyst combinations and photoreaction conditions allows the rapid development of an optimized photocatalytic system that achieves over 5000 turnovers with quantum yields greater than 34%. This material is available free of charge via the Internet at http://pubs.acs.org.

IC800988B